

FINITE-QUARK-MASS EFFECTS ON THE HIGGS PRODUCTION CROSS SECTION IN THE GLUON-GLUON FUSION CHANNEL

Dissertation

zur Erlangung des Doktorgrades an der Fakultät für Mathematik, Informatik und
Naturwissenschaften

Fachbereich Physik der Rheinisch-Westfälischen Technischen Hochschule

vorgelegt von

TOM CLAUS RUDOLF SCHELLENBERGER

Aachen

1. Juli 2025

Finite-Quark-Mass Effects on the Higgs Production Cross Section in the Gluon-Gluon Fusion Channel

© Tom Claus Rudolf Schellenberger 2025

GUTACHTER DER DISSERTATION:

Prof. Dr. Michał Czakon
Prof. Dr. Robert Harlander

ZUSAMMENSETZUNG DER PRÜFUNGSKOMMISSION:

Prof. Dr. Michał Czakon
Prof. Dr. Robert Harlander
TBA
TBA

VORSITZENDER DER PRÜFUNGSKOMMISSION:

TBA

DATUM DER DISPUTATION:

TBA

DEKAN DER FAKULTÄT MIN:

Prof. Dr. Carsten Honerkamp

ABSTRACT

This is my Abstract

ZUSAMMENFASSUNG

Dies ist meine Zusammenfassung

ACKNOWLEDGMENTS

Here is where I thank god.

PUBLICATIONS

During my PhD studies, I co-authored the following publications:

- [1] Michał Czakon, Felix Schmelter, and Tom Schellenberger. “Revisiting the double-soft asymptotics of one-loop amplitudes in massless QCD.” In: *JHEP* 04 (2023), p. 065. DOI: [10.1007/JHEP04\(2023\)065](#). arXiv: [2211.06465 \[hep-ph\]](#)
- [2] Michał Czakon, Felix Schmelter, and Tom Schellenberger. “Subleading effects in soft-gluon emission at one-loop in massless QCD.” In: *JHEP* 12 (2023), p. 126. DOI: [10.1007/JHEP12\(2023\)126](#). arXiv: [2307.02286 \[hep-ph\]](#)
- [3] Michał Czakon et al. “Top-Bottom Interference Contribution to Fully Inclusive Higgs Production.” In: *Phys. Rev. Lett.* 132.21 (2024), p. 211902. DOI: [10.1103/PhysRevLett.132.211902](#). arXiv: [2312.09896 \[hep-ph\]](#)
- [4] Michał Czakon et al. “Quark mass effects in Higgs production.” In: *JHEP* 10 (2024), p. 210. DOI: [10.1007/JHEP10\(2024\)210](#). arXiv: [2407.12413 \[hep-ph\]](#)

Among these, only the last two are directly relevant to this dissertation.

CONTENTS

1	Introduction	1
2	The Standard Model of Particle Physics	3
2.1	Electroweak Symmetry breaking	3
2.2	Cross Sections	7
2.2.1	The Hard Scattering Amplitude	8
2.2.2	The Parton Distribution Functions	10
2.2.3	The Phase-Space Integration	13
3	The Higgs as a Window to New Physics	17
3.1	Stability of the Higgs Potential	17
3.2	The Hierarchy Problem	17
4	Hadronic Higgs Production	19
4.1	The Leading-Order Cross Section	19
4.2	The Heavy-Top Limit	19
4.3	Higher-Order Corrections	19
4.4	Theory Status	19
5	Computational Details	21
5.1	Computing the Amplitudes	21
5.1.1	The Real-Real Corrections	21
5.1.2	The Real-Virtual Corrections	21
5.1.3	The Virtual-Virtual Corrections	21
5.2	$\overline{\text{MS}}$ -scheme	21
5.3	The 4-Flavour Scheme	21
5.4	Performing the Phase-Space Integration	21
6	Results and Discussion	23
6.1	Total Cross Section	23
6.1.1	Effects of Finite Top-Quark Masses	23
6.1.2	Effects of Finite Bottom-Quark Masses	23
6.2	Differential Cross Section	23
7	Conclusions	25
A	Feynman Rules of the Standard Model	27
	Bibliography	31

ACRONYMS

SM	Standard model
VEV	Vacuum expectation value
SSB	Spontaneous symmetry breaking
PDF	Parton distribution function
QCD	Quantum chromodynamics
RGE	Renormalization group equation
LO	Leading order
DR	Dimensional regularization
UV	Ultraviolet
IR	Infrared
LO	Leading order
NNLO	Next-to-next-to-leading order
OS	On-shell renormalization
RG	Renormalization group
RGE	Renormalization group equation
LHC	Large hadron collider
FS	Flavor scheme
MC	Monte-Carlo

NOTATION AND CONVENTIONS

- In this thesis, I will be using the *Einstein summation convention*, by which any index—be it a Lorentz, color or flavor index—which appears twice is implicitly summed over.

- I will be using natural units

$$\hbar = c = 1. \quad (0.1)$$

- The electron charge is

$$-e, \quad e > 0. \quad (0.2)$$

- The metric is

$$g_{\mu\nu} = \begin{pmatrix} 1 & & & \\ & -1 & & \\ & & -1 & \\ & & & -1 \end{pmatrix}. \quad (0.3)$$

- The normalization of the Levi-Civita anti-symmetric tensor $\epsilon_{\mu\nu\rho\sigma}$ is

$$\epsilon_{0123} = +1 \quad (0.4)$$

- The Pauli matrices are defined as

$$\sigma^1 \equiv \begin{pmatrix} 0 & 1 \\ 1 & 0 \end{pmatrix}, \quad \sigma^2 \equiv \begin{pmatrix} 0 & -i \\ i & 0 \end{pmatrix}, \quad \sigma^3 \equiv \begin{pmatrix} 1 & 0 \\ 0 & -1 \end{pmatrix}, \quad \tau^i \equiv \sigma^i. \quad (0.5)$$

1 | INTRODUCTION

General introductions

2.1 ELECTROWEAK SYMMETRY BREAKING

The standard model (SM) of particle physics is a theory describing all known matter and their fundamental interactions except for gravity. It unifies the electromagnetic, weak, and strong forces under a single theoretical framework. The matter content of the SM is classified into two primary groups: *fermions* and *bosons*. The fermions have spin 1/2, they are further subcategorized into *quarks* and *leptons*. Quarks participate in strong interactions, while leptons interact only via the electromagnetic and weak forces. In contrast, bosons have integer spin. There exists a single particle with spin 0, the *Higgs* boson, and four vector bosons, namely the gluon, the photon, and the *W* and *Z* boson. The vector bosons act as force carrier for the strong, the electromagnetic and the weak force respectively. Fermions are organized into three generations, with each generation containing two types of quarks (up-type and down-type) and two leptons (a charged lepton and its corresponding neutrino). These generations are shown in Fig. 2.1, along with their masses, charges, and spins.

The interactions between SM particles are described by a non-abelian gauge theory of the $SU(3)_C \times SU(2)_L \times U(1)_Y$ group. Here $SU(3)_C$ governs the strong interactions. It applies to all *colored* particles, i.e. quarks and gluons. The quarks transform under the fundamental representation of the $SU(3)_C$ group. $SU(2)_L \times U(1)_Y$ governs electroweak interactions. The $SU(2)_L$ transformation acts non-trivially only on *left-handed* fermions which form doublets

$$L_{iL} \equiv \begin{pmatrix} \nu_{iL} \\ l_{iL} \end{pmatrix}, \quad Q_{iL} \equiv \begin{pmatrix} u_{iL} \\ d_{iL} \end{pmatrix}, \quad (2.1)$$

$$\nu_i = (\nu_e, \nu_\mu, \nu_\tau), \quad l_i = (e, \mu, \tau), \quad u_i = (u, c, t), \quad d_i = (d, s, b).$$

The phase transformation $U(1)_Y$ acts on all particles except neutrinos according to their quantum number, the *hypercharge* Y . The symmetry is spontaneously broken to $SU(3)_C \times U(1)_Q$, where the $U(1)_Q$ group corresponds to gauge transformation of the electromagnetic interaction, hence the subscript Q for the *electric charge*. To ensure that the particles have the correct charges, the hypercharge must satisfy the *Gell-Mann–Nishijima relation*:

$$\frac{Y}{2} = Q - I^3. \quad (2.2)$$

With the particle charges displayed in Fig. 2.1 we then get

	L_{iL}	Q_{iL}	ν_{iR}	l_{iR}	u_{iR}	d_{iR}
$\frac{Y}{2}$	$-\frac{1}{2}$	$\frac{1}{6}$	0	-1	$\frac{2}{3}$	$-\frac{1}{3}$



Figure 2.1: Elementary particles of the SM. The was image generated with the help of Ref. [5].

The transformation properties of the gauge bosons is dictated by the covariance of the covariant derivative

$$D_\mu \equiv \partial_\mu - igA_\mu^a T_R^a - ig_2 W_\mu^a I^a + ig_Y \frac{Y}{2} B_\mu$$

$$T_R^a = \begin{cases} T^a & \text{for quarks,} \\ 0 & \text{for leptons,} \end{cases} \quad I^a = \begin{cases} \frac{\tau}{2} & \text{for left-handed fermions,} \\ 0 & \text{for right-handed fermions,} \end{cases} \quad (2.3)$$

where T^a and τ^a are the *Gell-Mann* and *Pauli* matrices.

Before spontaneous symmetry breaking, the Lagrangian which governs the evolution of all matter fields must be invariant under the $SU(3)_C \times SU(2)_L \times U(1)_Y$ gauge group. Up to a \mathbb{CP} violating term¹ the SM Lagrangian is the most general mass-dimension four Lagrangian for the described particle content

$$\mathcal{L}_{\text{SM}} = \mathcal{L}_G + \mathcal{L}_F + \mathcal{L}_Y + \mathcal{L}_H. \quad (2.4)$$

¹ The absence of the \mathbb{CP} violating term $\theta \frac{g^2}{64\pi^2} \epsilon^{\mu\nu\alpha\beta} F_{\mu\nu}^a F_{\alpha\beta}^a$ is an unsolved problem of particle physics, known as the strong CP problem.

The gauge-field Lagrangian \mathcal{L}_G describes the free propagation and in the case of the non-abelian groups $SU(3)_C$ and $SU(2)_L$ also the self-interaction of the gauge bosons. It is given by

$$\begin{aligned}\mathcal{L}_G &= -\frac{1}{4}G_{\mu\nu}^a G^{a\mu\nu} - \frac{1}{4}W_{\mu\nu}^a W^{a\mu\nu} - \frac{1}{4}B_{\mu\nu}B^{\mu\nu}, \\ G_{\mu\nu}^a &\equiv \partial_\mu A_\nu^a - \partial_\nu A_\mu^a + gf^{abc}A_\mu^b A_\nu^c, \\ W_{\mu\nu}^a &\equiv \partial_\mu W_\nu^a - \partial_\nu W_\mu^a + g_2\epsilon^{abc}W_\mu^b W_\nu^c, \\ B_{\mu\nu} &\equiv \partial_\mu B_\nu - \partial_\nu B_\mu.\end{aligned}\tag{2.5}$$

The propagation of the fermions and their interaction with the gauge bosons is described by

$$\mathcal{L}_F = \bar{L}_{iL}i\not{D}L_{iL} + \bar{\nu}_{iR}i\not{D}\nu_{iR} + \bar{l}_{iR}i\not{D}l_{iR} + \bar{Q}_{iL}i\not{D}Q_{iL} + \bar{u}_{iR}i\not{D}u_{iR} + \bar{d}_{iR}i\not{D}d_{iR}.\tag{2.6}$$

The Higgs field is a doublet of the $SU(2)_L$ group. We want the field to have a non-vanishing vacuum expectation value (VEV) to dynamically generate the fermion and boson masses. Of course, the vacuum cannot carry an electric charge, which means that the Higgs field must be electrically neutral along the direction of *spontaneous symmetry breaking* (SSB). We choose this to be the second component of the doublet. With the Gell-Mann–Nishijima relation we can then deduce that hypercharge of the doublet must be $Y = +1$. The Higgs doublet field thus takes the form

$$\Phi = \begin{pmatrix} \phi^+ \\ \phi^0 \end{pmatrix},\tag{2.7}$$

where the superscript indicates the electric charge.

In order to generate a non-vanishing VEV, the Higgs field must be in a potential with a global minimum away from zero. Hence, the only gauge invariant mass-dimension four Lagrangian we can construct is

$$\begin{aligned}\mathcal{L}_H &= (D_\mu\Phi)^\dagger (D^\mu\Phi) - V(\Phi) \\ V(\Phi) &= \lambda(\Phi^\dagger\Phi)^2 - \mu^2\Phi^\dagger\Phi, \quad \mu^2, \lambda > 0.\end{aligned}\tag{2.8}$$

The minimum of the Higgs potential V is at

$$\Phi_0^\dagger\Phi_0 = \frac{\mu^2}{2\lambda} \equiv \frac{v^2}{2} \neq 0.\tag{2.9}$$

After (SSB) we can expand the Higgs field around its minimum

$$\Phi = \begin{pmatrix} \phi^+ \\ \frac{1}{\sqrt{2}}(v + H + i\xi) \end{pmatrix}\tag{2.10}$$

The real scalar field H is the famous Higgs boson, whereas the fields ϕ^\pm and ξ are unphysical since they can always be eliminated through a gauge transformation (*would-be Goldstone bosons*). After inserting the expansion in the Higgs Lagrangian, the mass of the Higgs can be read off from its square term

$$m_H = \sqrt{2}\mu.\tag{2.11}$$

SSB enables the generation of vector boson masses without breaking the gauge symmetry explicitly. If we insert the expanded Higgs field in the Higgs Lagrangian, we get quadratic terms of the gauge boson fields

$$\begin{aligned}\mathcal{L}_H &\supseteq \frac{v^2}{2} \left\{ g_2^2 \begin{pmatrix} 0 & 1 \end{pmatrix} I^a I^b \begin{pmatrix} 0 \\ 1 \end{pmatrix} W_\mu^a W^{b\mu} - g_2 g_Y \begin{pmatrix} 0 & 1 \end{pmatrix} I^a \begin{pmatrix} 0 \\ 1 \end{pmatrix} W_\mu^a B^\mu + \frac{g_Y^2}{4} B_\mu B^\mu \right\} \\ &= \frac{v^2}{2} \left\{ \frac{g_2^2}{4} [(W^1)^2 + (W^2)^2] + \frac{1}{4} \begin{pmatrix} B^\mu & W^{3\mu} \end{pmatrix} \begin{pmatrix} g_Y^2 & g_Y g_2 \\ g_Y g_2 & g_2^2 \end{pmatrix} \begin{pmatrix} B_\mu \\ W_\mu^3 \end{pmatrix} \right\}.\end{aligned}\quad (2.12)$$

By diagonalizing the mass matrix we obtain the physical states

$$\begin{pmatrix} A_\mu^\gamma \\ Z_\mu \end{pmatrix} = \begin{pmatrix} \cos \theta_W & -\sin \theta_W \\ \sin \theta_W & \cos \theta_W \end{pmatrix} \begin{pmatrix} B_\mu \\ W_\mu^3 \end{pmatrix}, \quad \cos \theta_W = \frac{g_2}{\sqrt{g_Y^2 + g_2^2}}, \quad \sin \theta_W = \frac{g_Y}{\sqrt{g_Y^2 + g_2^2}}. \quad (2.13)$$

In this new basis, we have one massless boson A_μ^γ , which we identify as the photon and a charge neutral boson of mass

$$m_Z = \frac{v}{2} \sqrt{g_Y^2 + g_2^2}. \quad (2.14)$$

The vector bosons W^1 and W^2 are not eigenstates of the charge operator. We therefore define the new states

$$W_\mu^\pm = \frac{1}{\sqrt{2}} (W_\mu^1 \mp i W_\mu^2), \quad Q W_\mu^\pm = \pm W_\mu^\pm, \quad (2.15)$$

which are eigenstates of Q and have mass

$$m_W = \frac{v}{2} g_2. \quad (2.16)$$

Last but not least, we discuss the Yukawa sector of the SM Lagrangian. Before SSB, fermions cannot generate masses because a mass term would mix the left- and right-handed components of the fields, thereby breaking the chiral gauge symmetry. Here, once again, the Higgs field comes to the rescue: by coupling the fermions with the Higgs field through a Yukawa interaction²

$$\mathcal{L}_Y = - \left(y_{ij}^\nu \bar{L}_{iL} \Phi^c \nu_{jR} + y_{ij}^l \bar{L}_{iL} \Phi l_{jR} + y_{ij}^d \bar{Q}_{iL} \Phi d_{jR} + y_{ij}^u \bar{Q}_{iL} \Phi^c u_{jR} \right) + \text{h.c.}, \quad (2.17)$$

where Φ^c is the charge-conjugated field to Φ , we do not explicitly break the symmetry. However, after SSB this Lagrangian will generate exactly the required mixing between left- and right-handed fields to generate the fermion masses. The Yukawa-interaction matrices $y_{ij}^{\nu,l,d,u}$ can be shifted from the Yukawa sector to the fermion sector through a field redefinition. Indeed, if we apply the *singular value decomposition* of the Yukawa matrix

$$y = U_L^\dagger y_{\text{diag}} U_R, \quad \text{with} \quad (y_{\text{diag}})_{ij} = m_i \delta_{ij} \quad \text{and} \quad U_{L,R} \in \text{U}(3), \quad (2.18)$$

and redefine our fermion fields to be

$$f_{iR} \longrightarrow U_{Rij} f_{jR}, \quad f_{iL} \longrightarrow U_{Lij} f_{jL}, \quad f = \nu, l, u, d \quad (2.19)$$

the Yukawa Lagrangian becomes

$$\mathcal{L}_Y = - \sum_i \left(m_{\nu_i} \bar{\nu}_i \nu_i + m_{l_i} \bar{l}_i l_i + m_{u_i} \bar{u}_i u_i + m_{d_i} \bar{d}_i d_i \right) \left(1 + \frac{H}{v} \right). \quad (2.20)$$

² In the original formulation of the SM, there are no neutrino Yukawa interactions, since they were believed to be massless. Neutrino oscillation experiments have shown however, that neutrinos do in fact have finite masses.

As an immediate consequence, we observe that the Yukawa coupling of the Higgs to the fermions is proportional to the mass of that fermion. The field redefinition is a change from a flavor eigenbasis, which is diagonal in the couplings to the gauge bosons, to a mass eigenbasis. In the mass eigenbasis the part of fermion Lagrangian which contains the interaction to the electroweak gauge bosons after SSB is

$$\begin{aligned} \mathcal{L}_F \supset & \sum_f (-Q_f) e \bar{f}_i \not{A} f_i + \sum_f \frac{e}{\sin \theta_W \cos \theta_W} \bar{f}_i (I_f^3 \gamma^\mu P_L - \sin^2 \theta_W Q_f \gamma^\mu) f_i Z_\mu \\ & + \frac{e}{\sqrt{2} \sin \theta_W} \left(\bar{u}_i \gamma^\mu P_L (V_{\text{CKM}})_{ij} d_j W_\mu^+ + \bar{d}_i \gamma^\mu P_L (V_{\text{CKM}}^\dagger)_{ij} u_j W_\mu^- \right) \\ & + \frac{e}{\sqrt{2} \sin \theta_W} \left(\bar{\nu}_i \gamma^\mu P_L (V_{\text{PMNS}}^\dagger)_{ij} l_j W_\mu^+ + \bar{l}_i \gamma^\mu P_L (V_{\text{PMNS}})_{ij} \nu_j W_\mu^- \right). \end{aligned} \quad (2.21)$$

Here we identified the electromagnetic coupling constant

$$e = \frac{g_2 g_Y}{\sqrt{g_2^2 + g_Y^2}}, \quad (2.22)$$

as the factor in front of the photon interaction term. The operators $P_{L,R}$ are just the projectors onto the left- and right-handed components

$$P_{L,R} = \frac{1 \mp \gamma^5}{2}. \quad (2.23)$$

The *CKM* and *PMNS matrices*³ are the results of the field redefinitions

$$V_{\text{CKM}} \equiv U_L^{u\dagger} U_L^d, \quad V_{\text{PMNS}} \equiv U_L^{l\dagger} U_L^\nu. \quad (2.24)$$

Typically, one prefers to work in the mass eigenbasis of the quarks, while the neutrinos are kept in the flavor eigenbasis, in which case one encounters flavor changes (*neutrino oscillations*) through propagation. This is why the PMNS matrix is defined in terms of the complex conjugate of the CKM matrix equivalent in the lepton sector.

2.2 CROSS SECTIONS

Many of the great successes of the SM are its *cross section* predictions. The cross section is simply defined as the probability to create some final state from some initial state per unit of time per target particle divided by the incoming particle flux. This means that the cross section can be easily measured with a simple counting experiment. Experiments like **CMS** or **Atlas** do exactly that: they smash particles together and count how many times a certain final state was produced in some time interval. On the theory side, the cross section can be calculated with

$$d\sigma_{ij \rightarrow n} = \frac{1}{F} d\Phi_n |M_{ij \rightarrow n}|^2, \quad (2.25)$$

where F is the *flux factor*⁴

$$F \equiv 4p_1 \cdot p_2, \quad (2.26)$$

³ Named after Cabibbo, Kobayashi and Maskawa, and Pontecorvo, Maki, Nakagawa and Sakata.

⁴ In the following we assume that the initial state particles are massless.

$d\Phi_n$ is the *Lorentz invariant phase space measure*

$$d\Phi_n = \prod_{i=1}^n \frac{d^3\mathbf{q}_i}{(2\pi)^3 2q_i^0} (2\pi)^4 \delta^{(4)}\left(p_1 + p_2 - \sum_{i=1}^n q_i\right), \quad (2.27)$$

and M_{fi} is the *scattering amplitude* describing the hard interactions.

The computation of cross sections involves three basic steps:

1. the calculation of the hard scattering amplitude,
2. the phase-space integration,
3. and the convolution with *parton distribution functions* (PDFs).

In the following we will discuss them one-by-one.

2.2.1 The Hard Scattering Amplitude

The Hard Scattering Amplitude describes the transition probability from a certain initial state to a specific final state. Since the scattering is **hard**, the energy transfer between the particles during the scattering process is large compared to the QCD scale. This means we are in the perturbative regime of QCD, and we can perform an expansion in the coupling constant

$$M_{ij \rightarrow n} = \alpha_s^{n_{\text{Born}}} \left(M_{ij \rightarrow n}^{(0)} + \frac{\alpha_s}{\pi} M_{ij \rightarrow n}^{(1)} + \left(\frac{\alpha_s}{\pi} \right)^2 M_{ij \rightarrow n}^{(2)} + \mathcal{O}(\alpha_s^3) \right). \quad (2.28)$$

n_{Born} is the power of the coupling constant at *leading order* (LO). The coefficients of the series are calculable graphically using *Feynman rules*. These are the set of all allowed propagators and vertices together with the corresponding mathematical prescription. The Feynman rules for the complete SM are listed in Appendix A. To calculate the coefficient $M_{ij \rightarrow n}^{(l)}$ for a specific process, one just has to draw all possible (connected and amputated) Feynman diagrams with the initial state (i, j) and final state n , that contain $2(n_{\text{Born}} + l)$ vertices⁵. Then one uses the Feynman rules to get the mathematical translation, keeping in mind that momentum must be conserved at every vertex and also taking into account possible symmetry factors.

Starting from $M_{ij \rightarrow n}^{(1)}$, but for some processes, called *loop induced processes*, even from $M_{ij \rightarrow n}^{(0)}$, we will encounter loops in the diagrams. Inside a loop, the momentum of the edges cannot be uniquely determined through momentum conservation. In consequence, we have to leave the momentum unspecified and integrate over all values. Typically, it is the computation of these *loop integrals* that makes the calculation of hard scattering amplitudes so challenging. A plethora of powerful techniques has been developed over the years to tackle this daunting task. Still, the computation of loop integrals remains a highly active field and two-loop integrals with 5 or more scales are only just becoming available. A detailed description of modern techniques is beyond the scope of this thesis. For a comprehensive overview see Ref. [6].

Loop integrals are notorious for exhibiting divergences. To tame these, we introduce *regulators*, i.e. we introduce a parameter, such that the integral becomes function of that parameter with a singularity at the physical value. The most commonly used regularization scheme is

⁵ Quartic vertices are counted twice.

dimensional regularization (DR), here we make the loop-integral a function of the dimension by replacing

$$\int \frac{d^4 k}{(2\pi)^4} (\dots) \longrightarrow \bar{\mu}^{2\epsilon} \int \frac{d^d k}{(2\pi)^d} (\dots), \quad d \equiv 4 - 2\epsilon \in \mathbb{C}, \quad \gamma_E = 0.5772 \dots \quad (2.29)$$

The dimensionally regularized integral satisfies the usual integral properties like linearity, translation invariance and rescaling. The mass scale,

$$\bar{\mu}^2 = \frac{\mu^2}{4\pi} e^{\gamma_E} \quad (2.30)$$

was introduced to fix the mass dimension of the measure to 4, whereas the other factor was merely introduced to absorb some common factors of loop integrals. The physical limit then corresponds to $\epsilon \rightarrow 0$. A divergent integral in four dimensions will hence have ϵ -poles in DR. The poles are categorized as *ultraviolet* poles if their origin comes from large loop momenta, i.e. the four dimensional integral diverges for $k \rightarrow \infty$. Further we categorize poles as *infrared* poles if the singularity arises from loop momenta which are either soft ($k \rightarrow 0$) or *collinear* ($k \cdot p_i \rightarrow 0$) to one of the external massless legs. UV and IR singularities are mutually exclusive since they originate from different regions of the phase space. This means that the poles do not multiply. Therefore, we may only get a single UV pole per loop integration. The soft and collinear singularities are **not** exclusive, meaning that IR singularities can develop one double pole per loop integration.

The IR singularities cancel for inclusive observables as we shall discuss in detail in section 2.2.3. UV poles on the other hand, are removed through a method called *renormalization*. The basic idea here is that the fields, constants and masses we observe in nature are not the same as the one in our Lagrangian. Instead, they are related through a *renormalization constant*

$$\begin{aligned} W_\mu^{B,a} &= (Z_3^W)^{1/2} W_\mu^{R,a} \\ B_\mu^B &= (Z_3^Z)^{1/2} B_\mu^R \\ A_\mu^{B,a} &= (Z_3^A)^{1/2} A_\mu^{R,a} \\ \Phi^B &= (Z^\Phi)^{1/2} \Phi^R \\ Q_{iL}^B &= (Z_{2i}^L)^{1/2} Q_{iL}^R \\ u_{iR}^{B,a} &= (Z_{2i}^{u,R})^{1/2} u_{iR}^{B,a} \\ d_{iR}^{B,a} &= (Z_{2i}^{d,R})^{1/2} d_{iR}^{B,a} \\ g^B &= Z_g g^R \\ g_Y^B &= Z_Y g_Y^R \\ g_2^B &= Z_2 g_2^R \\ (\mu^2)^B &= Z_\mu (\mu^2)^R \\ \lambda^B &= Z_\lambda \lambda^R \\ y_{ij}^{d,B} &= Z_{y,ij}^d y_{ij}^{d,R} \\ y_{ij}^{u,B} &= Z_{y,ij}^u y_{ij}^{u,R} \end{aligned} \quad (2.31)$$

Here the B indicates the *bare* quantities appearing in the Lagrangian, and R denotes the renormalized ones we observe in nature. In the SM, it can be shown [7, 8] that we can choose

renormalization constants, such that *Green's functions*, i.e. vacuum expectation values of time ordered products of local renormalized fields, are free of UV divergences. Scattering amplitudes, generally do not depend on the unphysical fields, which is why the fields can be kept unrenormalized in this case. Since at LO Green's functions do not require renormalization, all renormalization constants are equal to the identity at this order.

The definition of the renormalization constants is not unique. Indeed, the renormalization constants were designed to absorb singularities, but the finite part is a priori unconstrained. We call a prescription which uniquely determines the renormalization constants a *renormalization scheme*. The most widely used renormalization scheme is the $\overline{\text{MS}}$ scheme. Here, beyond the leading 1 and a universal factor of $\bar{\mu}^{2\epsilon}$, the renormalization constants **only** consist of poles, i.e. the renormalization constants have the structure

$$Z_i(\alpha) = \bar{\mu}^{2\epsilon} \left(1 + \frac{z_1}{\epsilon} \frac{\alpha}{4\pi} + \left(\frac{z_{22}}{\epsilon^2} + \frac{z_{21}}{\epsilon} \right) \left(\frac{\alpha}{4\pi} \right)^2 + \dots \right). \quad (2.32)$$

$\overline{\text{MS}}$ -renormalized masses are generally different from the pole mass. The *on-shell renormalization* (OS) scheme, is an alternative to the $\overline{\text{MS}}$ scheme specifically designed, such that the renormalized mass matches the pole mass. It is therefore the suitable choice for external particles that are asymptotically free. Bare quantities are independent of the chosen renormalization scheme. The invariance under the change of the renormalization scheme defines a group, the *renormalization group* (RG). In the $\overline{\text{MS}}$ scheme, the change from one scale $\bar{\mu}$ to another defines a continuous subgroup of the RG. This means we can formulate the invariance in terms of a differential equation

$$0 = \frac{d}{d \log \mu} a^B = a^R \frac{d Z_a^{\overline{\text{MS}}}}{d \log \mu} + Z_a^{\overline{\text{MS}}} \frac{d a^R}{d \log \mu}, \quad (2.33)$$

where a could be a mass or a coupling. Eq. (2.33) is called the *renormalization group equation* (RGE) and it can be leveraged to determine the scale dependence, also called the *running*, of the observable.

The last step in calculating the hard scattering amplitude is applying the *Lehmann-Symanzik-Zimmermann* (LSZ) reduction formula. It relates the scattering amplitudes to Green's functions, and it is the reason why we only considered amputated Feynman diagrams. In practice, one just has to multiply each external field with the square root of the corresponding LSZ constant. These constants are defined as the proportionality factor between the propagator of the interacting and the free theory⁶. As such, they are numerically identical to the OS field renormalization constants.

2.2.2 The Parton Distribution Functions

In hadron collisions, the initial state is not made up of elementary particles, but are bound states thereof. This means that during an inelastic scattering event, the partons which take part in the short-range interaction only carry a fraction of the original hadron momentum

$$p_1 = x_1 P_1, \quad p_2 = x_2 P_2. \quad (2.34)$$

Here p_1 and p_2 are the momenta of the partons and P_1 and P_2 are the momenta of the hadrons. Since the momentum of the parton can not be larger than that of the hadron, $x_{1,2}$ is

⁶ The interacting field theory might have an additional continuous spectrum.

restricted to be less than one. Furthermore, since the energy of the parton must be positive the momentum fraction must also be positive. Otherwise, the momentum fraction is a priori unconstrained, we therefore integrate over all allowed values of x_1 and x_2

$$\begin{aligned} d\sigma_{H_1 H_2 \rightarrow n}(S) &= \int_0^1 dx_1 dx_2 f_{H_1, i}(x_1) f_{H_2, j}(x_2) d\hat{\sigma}_{ij \rightarrow n}(x_1 P_1, x_2 P_2, \mu_R) \\ &= \int_0^1 d\tau \mathcal{L}_{ij}(\tau) d\hat{\sigma}_{ij \rightarrow n}(\tau S, \mu_R) \end{aligned} \quad (2.35)$$

where $S = 2P_1 \cdot P_2$ is hadronic center of mass energy. $f_{H_k, i}(x_k)$ are the (unrenormalized) *parton distribution functions* (PDFs). They describe the probability of finding a parton i with momentum fraction x_k inside the hadron H_k . Lorentz invariance of the partonic cross section allowed us to conclude that it can only depend on the partonic center of mass energy

$$d\hat{\sigma}_{ij \rightarrow n}(x_1 P_1, x_2 P_2, \mu_R) = d\hat{\sigma}_{ij \rightarrow n}(x_1 x_2 S, \mu_R). \quad (2.36)$$

We then defined the partonic luminosity

$$\mathcal{L}_{ij}(\tau) \equiv (f_{H_1, i} \otimes f_{H_2, j})(\tau) \equiv \int_0^1 dx_1 dx_2 f_{H_1, i}(x_1) f_{H_2, j}(x_2) \delta(\tau - x_1 x_2), \quad (2.37)$$

to arrive at the second line of Eq. (2.35).

At this stage the partonic cross section can still exhibit singularities whenever a final state parton becomes collinear to one of the initial state partons. At LO for example the divergence reads

$$d\hat{\sigma}_{ab \rightarrow cX}(s, \mu_R) \Big|_{\text{div.}} = -\frac{\alpha_s}{2\pi} \frac{1}{\epsilon} \int_0^1 dz \left(P_{db}^{(0)}(z) d\hat{\sigma}_{ad \rightarrow X}(zs, \mu_R) + P_{da}^{(0)}(z) d\hat{\sigma}_{db \rightarrow X}(zs, \mu_R) \right), \quad (2.38)$$

where $P_{ij}^{(0)}$ are the LO *Altarelli-Parisi splitting kernels*.

We want to absorb these collinear singularities into the PDFs, a process called *initial-state-collinear renormalization*, by defining the renormalized PDFs

$$f_{H, i}(x) \equiv (Z_{ij}(\cdot, \mu_F) \otimes f_{H, j}(\cdot, \mu_F))(x). \quad (2.39)$$

Beyond the pole, the renormalization constants are generally scheme dependent. From Eq. (2.38) we see that the $\overline{\text{MS}}$ renormalization constant at NLO must read

$$Z_{ij}(z, \mu_R, \mu_F) = \delta(1-z) \delta_{ij} + \frac{\alpha_s}{2\pi} \frac{1}{\epsilon} P_{ij}^{(0)}(z) + \mathcal{O}(\alpha_s^2), \quad (2.40)$$

since now the sum

$$d\sigma_{H_1 H_2 \rightarrow cX} + d\sigma_{H_1 H_2 \rightarrow X} \quad (2.41)$$

is guaranteed to be free of divergences when c becomes collinear to the initial state. Since the initial state collinear divergences are of a completely different origin than the UV divergences, we introduced a new scale μ_F , called the factorization scale.

The factorization theorem (2.35) is central in the SM as it tells us that the PDFs are universal quantities, i.e. they are not specific to any one process. It is a postulate of the parton model, in which hadrons are thought of as collection of the free elementary particles. In QCD however, the theorem requires proof [11]! The PDF for all light partons are displayed in Fig. 2.2. PDFs describe long range interactions, a regime in which QCD is non-perturbative. As such, PDFs

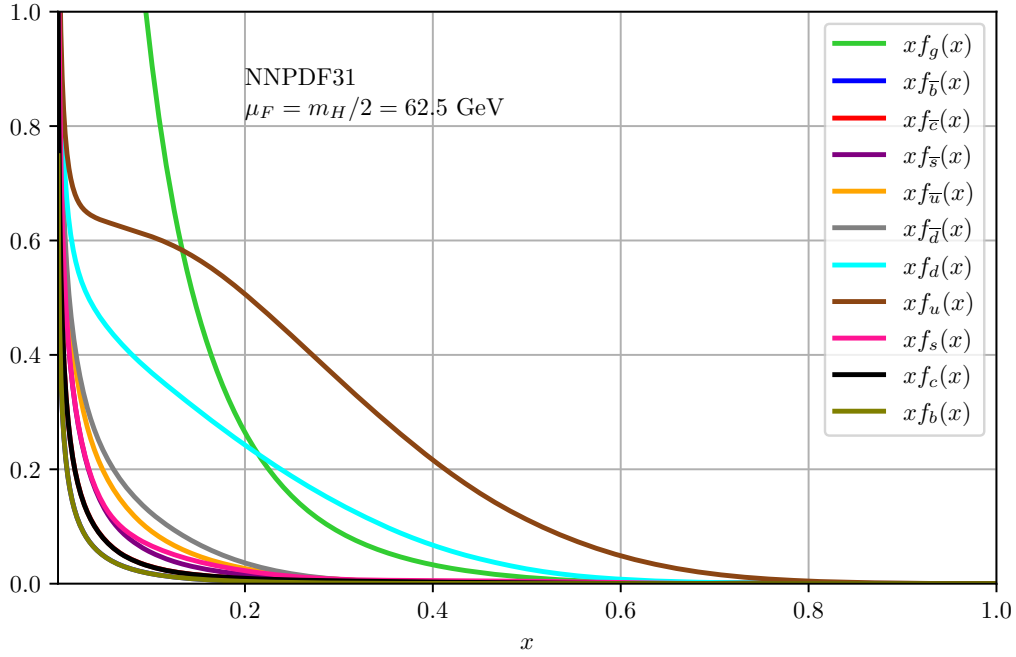


Figure 2.2: The various PDFs multiplied by x as a function of x . The plot was created using the LHAPDF6 [9] interface to the NNPDF31_nnlo_as_0118 [10] PDF set at a scale of $\mu_F = m_H/2$.

are non-perturbative objects which have to be measured in experiments or be calculated non-perturbatively, e.g. on the lattice.

The scale μ_F marks the boundary, over which we treat interactions perturbatively. This scale is unphysical in the sense that it is not a parameter in our theory, nor can it be measured in an experiment. As usual we can apply the RGE to determine the running of the renormalized PDFs.

$$0 = \frac{d}{d \ln \mu_F} f_{H,i}(x) = \frac{d}{d \ln \mu_F} (Z_{ij} \otimes f_{H,j}(\cdot, \mu_F))(x). \quad (2.42)$$

This can be rewritten to

$$\begin{aligned} \frac{df_{H,i}(x, \mu_F)}{d \ln \mu_F} &= 2\alpha_s \left(Z_{ij}^{-1} \otimes \frac{dZ_{jk}^{(1)}}{d\alpha_s} \otimes f_{H,k}(\cdot, \mu_F) \right) (x, \mu_F) \\ &= \frac{\alpha_s}{\pi} \left(P_{ij}^{(0)} \otimes f_{H,j}(\cdot, \mu_F) \right) (x) + \mathcal{O}(\alpha_s^2), \end{aligned} \quad (2.43)$$

where $Z_{ij}^{(1)}$ is the residue of the renormalization constant. So even though the PDFs are non-perturbative, their dependence on the factorization scale is. Eq. (2.43) is the famous *Dokshitzer-Gribov-Lipatow-Altarelli-Parisi-evolution equation* (DGLAP equations) [12, 13, 14].

Up until now, we always treated the partons inside the hadrons as massless, hence we had to deal with real collinear singularities. In reality, all the quarks have finite masses, such that the phase-space integration only yields logarithmic mass enhancements instead of singularities. The DGLAP equations then automatically resum these logarithms. Since for most applications at the LHC, the typical hard scattering scale is orders of magnitudes larger than all quark masses but the top quark mass, it is typically a good idea to treat them as massless partons,

as the appearance of the large logarithms would otherwise completely destroy the perturbative convergence. The downside here is that now the quarks must also be treated as massless inside the hard scattering element. If the scattering element is sensitive to the mass, e.g. if we consider couplings to the Higgs, then these effects might be lost. Generally speaking, if the number of quarks which we treat as massless constituents of the hadron defines our flavor scheme (FS). That means if the lightest four flavors are treated as massless, while the bottom and the top quark are considered massive, then we are using in the 4FS. Analogously, we are working in the 5FS if the bottom quark is also considered massive and so on.

2.2.3 The Phase-Space Integration

Even after renormalization and collinear renormalization can the amplitude exhibit poles. The scattering amplitude in and of itself is not a physical observable, therefore we can not expect it to be finite. What we can observe are cross sections. We can get the cross section by applying Eq. (2.25), i.e. performing a phase space integration over the scattering amplitude. Even then, we find that the cross section is not guaranteed to be finite. The reason is that the Born process is indistinguishable from processes with additional infrared radiation. Indeed, no matter how good your detector is, below a certain resolution, one will no longer be able to detect a very soft photon or distinguish to highly collinear jets. Hence, computing a cross section with a fixed final state does not make physical sense. Instead, we have to consider sufficiently inclusive observables—so called *IR-safe observables*. For these, Kinoshita, Lee and Nauenberg proved that in unitary theories all IR singularities cancel [15, 16]. An example of an observable which is trivially IR safe is the fully inclusive cross section

$$\hat{\sigma}_{ij \rightarrow n+X} = \sum_{k=1}^{\infty} \hat{\sigma}_{ij \rightarrow n+k}, \quad \text{for } \hat{\sigma}_{ij \rightarrow n}^{(0)} \text{ finite}, \quad (2.44)$$

where $n+k$ indicates that in addition to the final state n we now have k massless particles of whatever flavor. In perturbation theory, the infinite sum is terminated at the desired order and each order

$$\hat{\sigma}_{ij \rightarrow n+X}^{(l)} = \sum_{k=0}^l \hat{\sigma}_{ij \rightarrow n+k}^{(l-k)}, \quad (2.45)$$

will be finite. The required partonic cross sections for Higgs production in the gluon fusion channel at various perturbative orders, are pictorially represented in Fig. 2.3.

For practical applications, the appearance of IR singularities pose an immense challenge, as the divergences prohibit a direct evaluation of the phase-space integrals. Instead, we once again have to introduce regulators to even make the integrals well-defined. Numerous techniques have been developed over the years to compute the phase-space integrals. They can be generally categorized into two main types: *Analytic methods*, and *numerical methods*. As the name suggests, in the former class, the phase-space integrals are solved analytically. One noteworthy member of this class is the *reverse-unitarity method* [17], which was first applied to Higgs production in the gluon fusion channel. The method uses unitarity, to rewrite the phase-space integrals in terms of loop integrals over cut-propagators. One can then apply the remarkable techniques developed for Feynman integrals to these phase-space integrals and solve them analytically. The mayor downside of this approach is that it is highly process and observable dependent, meaning that for every process and every observable we have to start over from scratch. Furthermore, by the very nature of the method, you are always restricted to inclusive jet observables. It has been successfully applied to Higgs-rapidity and $-p_T$ distributions [18].

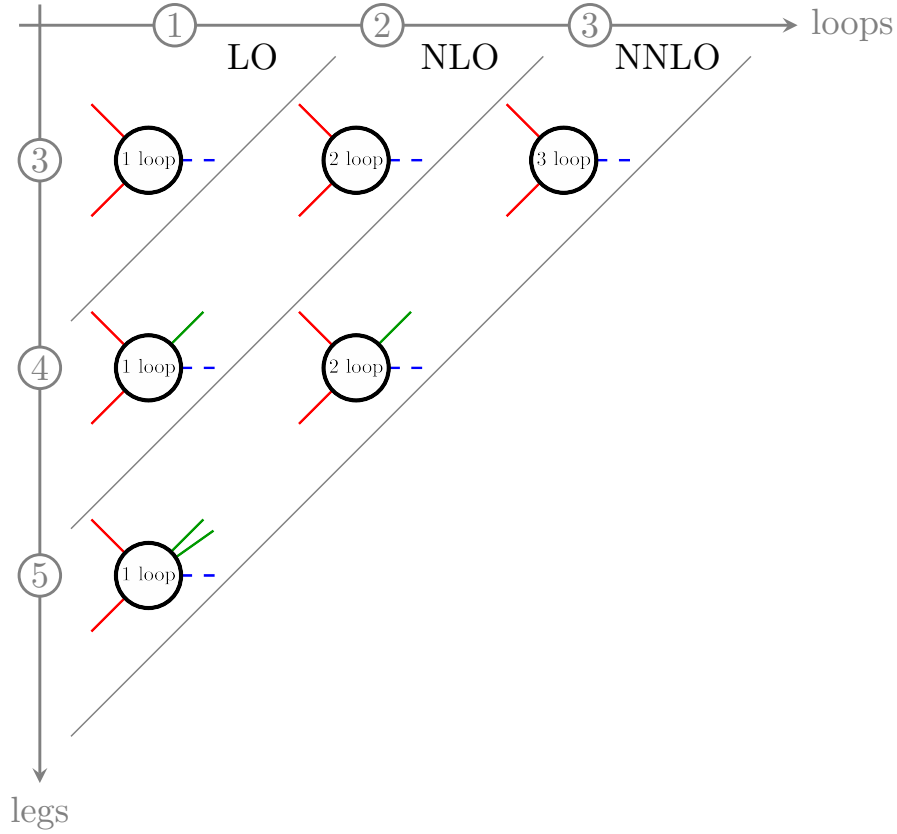


Figure 2.3: Pictorial representation of the needed partonic cross sections at various perturbative orders of the fully inclusive hadronic cross section. The graphic shows the example of Higgs production in the gluon fusion channel.

Among the numerical methods, there are two mayor types: *slicing* and *subtraction methods*. The former relies on a variable that isolates the IR-sensitive region of the phase space. Consider once again the example of Higgs production. Then the IR-sensitive region of the phase-space is going to be at $p_T \rightarrow 0$, where p_T is the transverse momentum of the Higgs, and the phase-space integral can be decomposed into

$$\int_0^{p_T} dk_T d\hat{\sigma}_{ij \rightarrow H+c} = \int_0^{p_T^{\text{cut}}} dk_T d\hat{\sigma}_{ij \rightarrow H+c} + \int_{p_T^{\text{cut}}}^{p_T} dk_T d\hat{\sigma}_{ij \rightarrow H+c}. \quad (2.46)$$

The first integral on the right-hand side is now finite and can be computed numerically, e.g. using *Monte-Carlo* (MC) techniques. If we choose p_T^{cut} small enough, then we can approximate the integrand in the second integral, by its IR factorization and solve the integral analytically. The pole of the integral should then cancel against the poles in the virtual integration and the counter term from collinear renormalization. The mayor advantage of this method is its simplicity. One big downside is its dependence on the unphysical cutoff scale. Ideally it is chosen very small, such that the approximation introduces little to no error. But if chosen too small, the integrations will have huge logarithmic enhancements which can easily spoil the numerical precision. Another disadvantage is that not all processes or observables have easily identifiable slicing variables, or the analytic integration is very challenging. For example, p_T slicing only works for color singlet production, indeed if we have a jet in the final state, we

can encounter collinear divergences also at finite transverse momenta of the jet. Instead, for final state jets, a possible slicing variable is the N -jettiness

$$\mathcal{T}_N \equiv \sum_k \min_i \left\{ \frac{2p_i \cdot q_k}{Q_i} \right\}, \quad (2.47)$$

with N , the number of jets, q_k , the momenta of the unresolved partons, p_i , the momenta of the resolved jets, and Q_i a normalization factor which can for example be set to the jet energy. However, the analytic integration becomes highly non-trivial and is a matter of active research. Currently, the N -jettiness beam functions are known at N³LO [19], the 0-jettiness soft function is known at N³LO [20, 21] and NNLO 1-jettiness soft functions and jet functions are also known [22, 23, 24, 25].

Subtraction methods on the other hand, work by subtracting the infrared limits on the integrand level. In the *Frixione-Kunszt-Signer subtraction scheme* (FKS subtraction scheme) or the *sector improved residue subtraction scheme* [26] one first isolates the IR divergence by introducing *selector functions*. These are functions which approach the identity in their corresponding limit, while they are zero whenever a limit is approached which does not correspond to that selector function. For a single unresolved parton, a possible selector function is

$$\mathcal{S}_{n+1,k} \equiv \frac{1}{d_{n+1,k}} \left(\sum_k \frac{1}{d_{n+1,k}} \right)^{-1}, \quad \text{where} \quad d_{n+1,k} \equiv \left(\frac{E_{n+1}}{\sqrt{\hat{s}}} \right)^\alpha (1 - \cos \theta_{n+1,k})^\beta. \quad (2.48)$$

The first index $n + 1$ is the index of the unresolved parton, while the second index is the index of the reference parton. E_{n+1} denotes the energy of the unresolved parton, this factor is therefore to identify soft singularities. Consequently, the power α can be set to zero if the unresolved parton is a quark. Other than that the powers must be strictly positive $\alpha, \beta > 0$. If we $n + 1$ becomes collinear to one of the other partons, say parton i , then the selector function $\mathcal{S}_{n+1,i}$ will approach one. And since the selector functions are strictly positive and form a decomposition of unity

$$\sum_k \mathcal{S}_{n+1,k} = 1, \quad (2.49)$$

all other selector functions will go to zero simultaneously. We can then write the real emission cross section as

$$\hat{\sigma}_{ij \rightarrow n+u} = \frac{1}{F} \sum_k \int d\Phi_{n+1} |M_{ij \rightarrow n+u}^{(0)}|^2 \mathcal{S}_{n+1,k}. \quad (2.50)$$

Now say we found a way to factorize the phase space, such that the infrared limits of a specific sector, defined by a selector function, are isolated (see for example Ref. [27]). Then in each sector, we will have two unit integrations over ξ and η which parameterize the soft and collinear limit respectively, i.e. if $\xi \rightarrow 0$, then the momentum of the unresolved parton goes to zero and if $\eta \rightarrow 0$, the unresolved parton will become collinear to the reference momentum of that sector. The amplitude In the end we will end up with integrals of the form

$$\int_0^1 \frac{d\eta}{\eta^{1+\epsilon}} \frac{d\xi}{\xi^{1+2\epsilon}} f(\eta, \xi, \dots), \quad (2.51)$$

where f is regular in the limits $\eta, \xi \rightarrow 0$, and we used the fact that the amplitude has the singular scaling $|M_{ij \rightarrow n+u}^{(0)}|^2 = \mathcal{O}(\xi^{-2}) \mathcal{O}(\eta^{-1})$.

3 | THE HIGGS AS A WINDOW TO NEW PHYSICS

3.1 STABILITY OF THE HIGGS POTENTIAL

3.2 THE HIERARCHY PROBLEM

4 | HADRONIC HIGGS PRODUCTION

4.1 THE LEADING-ORDER CROSS SECTION

Here I compute the leading-order cross section for Higgs Production in the gluon-gluon fusion channel.

4.2 THE HEAVY-TOP LIMIT

Here I explain the heavy-top limit.

4.3 HIGHER-ORDER CORRECTIONS

Here I outline how to perform higher order corrections.

4.4 THEORY STATUS

Here I describe what is already known about the gluon-gluon fusion channel. I explain the theory uncertainties.

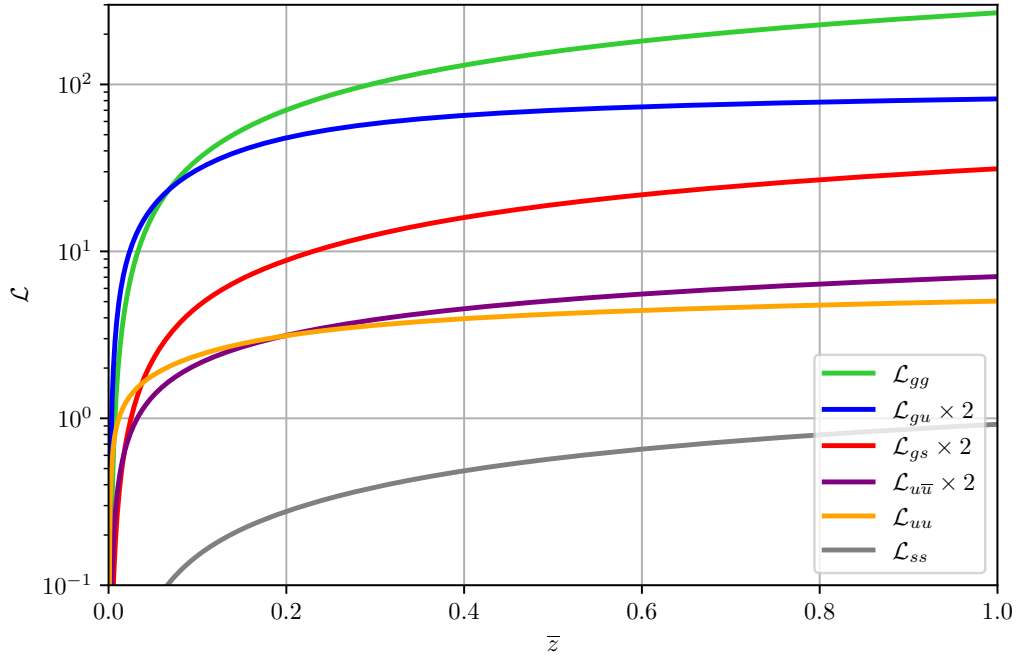


Figure 4.1: Illustration of the partonic luminosity of parton i and j . We choose exemplary parton combinations to represent gluon–gluon, gluon–valence-quark, gluon–sea-quark, valence-quark–sea-quark, valence-quark–valence-quark and sea-quark–sea-quark luminosities. For the luminosity of two different partons we include a factor 2 to account for the different flavor permutations. The luminosity was calculated using the LHAPDF6 [9] interface to the NNPDF31_nnlo_as_0118 [10] PDF set at a scale of $\mu_F = m_H/2$ with a fixed collider energy of $\sqrt{S} = 13$ TeV.

5 | COMPUTATIONAL DETAILS

Description of this chapter.

5.1 COMPUTING THE AMPLITUDES

Here I

5.1.1 The Real-Real Corrections

5.1.2 The Real-Virtual Corrections

5.1.3 The Virtual-Virtual Corrections

5.2 $\overline{\text{MS}}$ -SCHEME

5.3 THE 4-FLAVOUR SCHEME

5.4 PERFORMING THE PHASE-SPACE INTEGRATION

6 | RESULTS AND DISCUSSION

Description of this chapter.

6.1 TOTAL CROSS SECTION

6.1.1 Effects of Finite Top-Quark Masses

6.1.2 Effects of Finite Bottom-Quark Masses

6.2 DIFFERENTIAL CROSS SECTION

7 | CONCLUSIONS

Here are my conclusions.

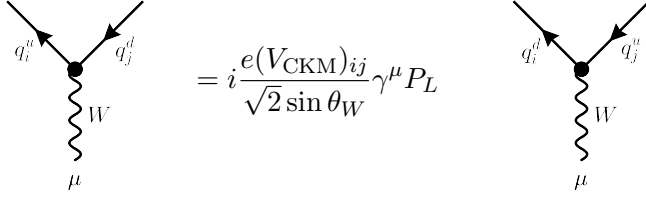
In this chapter we list all Feynman rules of the SM. We choose to work in a unitary gauge, meaning that the all Goldstone-bosons decouple and there are no unphysical particles in the electroweak sector. In the QCD sector, we work in the R_ξ gauge, i.e. we have unphysical particles in the form of *Faddeev-Popov ghosts*. If not otherwise specified, the momenta on every line are defined as incoming.

Propagators:

$$\begin{aligned}
 a, \mu \quad \text{---} \overline{\text{---}} \overline{\text{---}} \overline{\text{---}} \overline{\text{---}} \overline{\text{---}} \overline{\text{---}} \overline{\text{---}} \overline{\text{---}} \text{---} \quad b, \nu &= i \frac{\delta^{ab}}{k^2 + i0^+} \left[-g_{\mu\nu} + (1 - \xi) \frac{k_\mu k_\nu}{k^2 + i0^+} \right] \\
 i \quad \text{---} \overline{\text{---}} \overline{\text{---}} \overline{\text{---}} \overline{\text{---}} \text{---} \quad j &= i \delta_{ij} \frac{\not{k} + m}{k^2 - m^2 + i0^+} \\
 \text{---} \overline{\text{---}} \overline{\text{---}} \overline{\text{---}} \overline{\text{---}} \text{---} &= i \frac{1}{k^2 - m_H^2 + i0^+} \\
 \mu \quad \text{---} \overline{\text{---}} \overline{\text{---}} \overline{\text{---}} \overline{\text{---}} \text{---} \quad \nu &= i \frac{-g_{\mu\nu}}{k^2 + i0^+} \\
 \mu \quad \text{---} \overline{\text{---}} \overline{\text{---}} \overline{\text{---}} \overline{\text{---}} \text{---} \quad \nu &= i \frac{1}{k^2 - m_W^2 + i0^+} \left(-g_{\mu\nu} + \frac{k_\mu k_\nu}{m_W^2 + i0^+} \right) \\
 \mu \quad \text{---} \overline{\text{---}} \overline{\text{---}} \overline{\text{---}} \overline{\text{---}} \text{---} \quad \nu &= i \frac{1}{k^2 - m_Z^2 + i0^+} \left(-g_{\mu\nu} + \frac{k_\mu k_\nu}{m_Z^2 + i0^+} \right) \\
 a \quad \text{---} \overline{\text{---}} \overline{\text{---}} \overline{\text{---}} \overline{\text{---}} \text{---} \quad b &= i \frac{\delta^{ab}}{k^2 + i0^+}
 \end{aligned}$$

Fermion–Gauge-Boson Vertices:

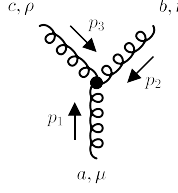
$$\begin{aligned}
 \begin{array}{c} i \quad \nearrow \\ \searrow \quad j \\ \text{---} \overline{\text{---}} \overline{\text{---}} \overline{\text{---}} \overline{\text{---}} \text{---} \\ a, \mu \end{array} &= ig \gamma^\mu T_{ij}^a \\
 \begin{array}{c} \nearrow \quad \searrow \\ \text{---} \overline{\text{---}} \overline{\text{---}} \overline{\text{---}} \overline{\text{---}} \text{---} \\ \mu \end{array} &= -ie \gamma^\mu Q \\
 \begin{array}{c} a \quad \nearrow \\ \searrow \quad b \\ \text{---} \overline{\text{---}} \overline{\text{---}} \overline{\text{---}} \overline{\text{---}} \text{---} \\ c, \mu \end{array} &= g f^{abc} p^\mu \\
 \begin{array}{c} \nearrow \quad \searrow \\ \text{---} \overline{\text{---}} \overline{\text{---}} \overline{\text{---}} \overline{\text{---}} \text{---} \\ \mu \end{array} &= i \frac{e}{\sin \theta_W \cos \theta_W} \gamma^\mu \\
 &\quad \times (I^3 P_L - Q \sin^2 \theta_W)
 \end{aligned}$$



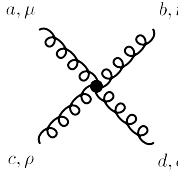
$$= i \frac{e(V_{\text{CKM}})_{ij}}{\sqrt{2} \sin \theta_W} \gamma^\mu P_L$$

$$= i \frac{e(V_{\text{CKM}})^*_{ji}}{\sqrt{2} \sin \theta_W} \gamma^\mu P_L$$

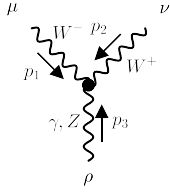
Gauge-Boson Self Interactions:



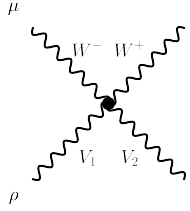
$$= g f^{abc} ((p_1^\rho - p_2^\rho) g^{\mu\nu} + (p_2^\mu - p_3^\mu) g^{\nu\rho} + (p_3^\nu - p_1^\nu) g^{\rho\mu})$$



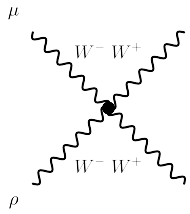
$$= -ig^2 (f^{abe} f^{cde} (g^{\mu\rho} g^{\nu\sigma} - g^{\mu\sigma} g^{\nu\rho}) + f^{ace} f^{bde} (g^{\mu\nu} g^{\rho\sigma} - g^{\mu\sigma} g^{\nu\rho}) + f^{ade} f^{bce} (g^{\mu\nu} g^{\rho\sigma} - g^{\mu\rho} g^{\nu\sigma}))$$



$$= i \frac{e}{\sin \theta_W} ((p_1^\rho - p_2^\rho) g^{\mu\nu} + (p_2^\mu - p_3^\mu) g^{\nu\rho} + (p_3^\nu - p_1^\nu) g^{\rho\mu}) \times \begin{cases} -\sin \theta_W & \text{for } \gamma \\ \cos \theta_W & \text{for } Z \end{cases}$$



$$= i \frac{e^2}{\sin^2 \theta_W} (g^{\mu\sigma} g^{\nu\rho} + g^{\mu\rho} g^{\nu\sigma} - 2g^{\mu\nu} g^{\rho\sigma}) \times \prod_{i=1}^2 \begin{cases} -\sin \theta_W & \text{if } V_i = \gamma \\ \cos \theta_W & \text{if } V_i = Z \end{cases}$$



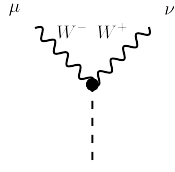
$$= i \frac{e^2}{\sin^2 \theta_W} (2g^{\mu\rho} g^{\nu\sigma} - g^{\mu\nu} g^{\rho\sigma} - g^{\mu\sigma} g^{\nu\rho})$$

Higgs Interactions:

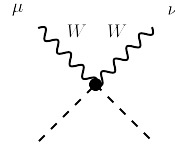


$$= -i \frac{m_q}{v} \delta_{ij}$$

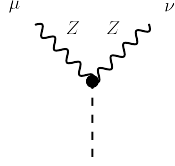

$$= -i \frac{3m_H^2}{v}$$



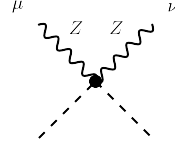
$$= i \frac{e}{\sin \theta_W} m_W g^{\mu\nu}$$



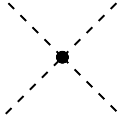
$$= i \frac{e^2}{2 \sin^2 \theta_W} g^{\mu\nu}$$



$$= i \frac{e}{\sin \theta_W \cos \theta_W} m_Z g^{\mu\nu}$$



$$= i \frac{e^2}{2 \sin^2 \theta_W \cos^2 \theta_W} g^{\mu\nu}$$



$$= -i \frac{3m_H^2}{v^2}$$

BIBLIOGRAPHY

- [1] Michał Czakon, Felix Schlenker, and Tom Schellenberger. “Revisiting the double-soft asymptotics of one-loop amplitudes in massless QCD.” In: *JHEP* 04 (2023), p. 065. DOI: [10.1007/JHEP04\(2023\)065](https://doi.org/10.1007/JHEP04(2023)065). arXiv: [2211.06465](https://arxiv.org/abs/2211.06465) [hep-ph].
- [2] Michał Czakon, Felix Schlenker, and Tom Schellenberger. “Subleading effects in soft-gluon emission at one-loop in massless QCD.” In: *JHEP* 12 (2023), p. 126. DOI: [10.1007/JHEP12\(2023\)126](https://doi.org/10.1007/JHEP12(2023)126). arXiv: [2307.02286](https://arxiv.org/abs/2307.02286) [hep-ph].
- [3] Michał Czakon et al. “Top-Bottom Interference Contribution to Fully Inclusive Higgs Production.” In: *Phys. Rev. Lett.* 132.21 (2024), p. 211902. DOI: [10.1103/PhysRevLett.132.211902](https://doi.org/10.1103/PhysRevLett.132.211902). arXiv: [2312.09896](https://arxiv.org/abs/2312.09896) [hep-ph].
- [4] Michał Czakon et al. “Quark mass effects in Higgs production.” In: *JHEP* 10 (2024), p. 210. DOI: [10.1007/JHEP10\(2024\)210](https://doi.org/10.1007/JHEP10(2024)210). arXiv: [2407.12413](https://arxiv.org/abs/2407.12413) [hep-ph].
- [5] Izaak Neutelings. *Izaak neutelings*. Mar. 2024. URL: https://tikz.net/sm_particles/.
- [6] Stefan Weinzierl. *Feynman Integrals. A Comprehensive Treatment for Students and Researchers*. UNITEXT for Physics. Springer, 2022. ISBN: 978-3-030-99557-7, 978-3-030-99560-7, 978-3-030-99558-4. DOI: [10.1007/978-3-030-99558-4](https://doi.org/10.1007/978-3-030-99558-4). arXiv: [2201.03593](https://arxiv.org/abs/2201.03593) [hep-th].
- [7] Gerard 't Hooft. “Renormalizable Lagrangians for Massive Yang-Mills Fields.” In: *Nucl. Phys. B* 35 (1971). Ed. by J. C. Taylor, pp. 167–188. DOI: [10.1016/0550-3213\(71\)90139-8](https://doi.org/10.1016/0550-3213(71)90139-8).
- [8] Gerard 't Hooft and M. J. G. Veltman. “Regularization and Renormalization of Gauge Fields.” In: *Nucl. Phys. B* 44 (1972), pp. 189–213. DOI: [10.1016/0550-3213\(72\)90279-9](https://doi.org/10.1016/0550-3213(72)90279-9).
- [9] Andy Buckley et al. “LHAPDF6: parton density access in the LHC precision era.” In: *Eur. Phys. J. C* 75 (2015), p. 132. DOI: [10.1140/epjc/s10052-015-3318-8](https://doi.org/10.1140/epjc/s10052-015-3318-8). arXiv: [1412.7420](https://arxiv.org/abs/1412.7420) [hep-ph].
- [10] Richard D. Ball et al. “Parton distributions from high-precision collider data.” In: *Eur. Phys. J. C* 77.10 (2017), p. 663. DOI: [10.1140/epjc/s10052-017-5199-5](https://doi.org/10.1140/epjc/s10052-017-5199-5). arXiv: [1706.00428](https://arxiv.org/abs/1706.00428) [hep-ph].
- [11] John C. Collins, Davison E. Soper, and George F. Sterman. “Factorization of Hard Processes in QCD.” In: *Adv. Ser. Direct. High Energy Phys.* 5 (1989), pp. 1–91. DOI: [10.1142/9789814503266_0001](https://doi.org/10.1142/9789814503266_0001). arXiv: [hep-ph/0409313](https://arxiv.org/abs/hep-ph/0409313).
- [12] Yuri L. Dokshitzer. “Calculation of the Structure Functions for Deep Inelastic Scattering and e^+e^- Annihilation by Perturbation Theory in Quantum Chromodynamics.” In: *Sov. Phys. JETP* 46 (1977), pp. 641–653.
- [13] V. N. Gribov and L. N. Lipatov. “Deep inelastic $e p$ scattering in perturbation theory.” In: *Sov. J. Nucl. Phys.* 15 (1972), pp. 438–450.
- [14] Guido Altarelli and G. Parisi. “Asymptotic Freedom in Parton Language.” In: *Nucl. Phys. B* 126 (1977), pp. 298–318. DOI: [10.1016/0550-3213\(77\)90384-4](https://doi.org/10.1016/0550-3213(77)90384-4).
- [15] T. Kinoshita and A. Ukawa. “Mass Singularities of Feynman Amplitudes.” In: *Lect. Notes Phys.* 39 (1975). Ed. by Huzihiro Araki, pp. 55–58. DOI: [10.1007/BFb0013300](https://doi.org/10.1007/BFb0013300).

- [16] T. D. Lee and M. Nauenberg. “Degenerate Systems and Mass Singularities.” In: *Phys. Rev.* 133 (1964). Ed. by G. Feinberg, B1549–B1562. DOI: [10.1103/PhysRev.133.B1549](#).
- [17] Charalampos Anastasiou and Kirill Melnikov. “Higgs boson production at hadron colliders in NNLO QCD.” In: *Nucl. Phys. B* 646 (2002), pp. 220–256. DOI: [10.1016/S0550-3213\(02\)00837-4](#). arXiv: [hep-ph/0207004](#).
- [18] Falko Dulat et al. “Higgs-differential cross section at NNLO in dimensional regularisation.” In: *JHEP* 07 (2017), p. 017. DOI: [10.1007/JHEP07\(2017\)017](#). arXiv: [1704.08220 \[hep-ph\]](#).
- [19] Markus A. Ebert, Bernhard Mistlberger, and Gherardo Vita. “ N -jettiness beam functions at N³LO.” In: *JHEP* 09 (2020), p. 143. DOI: [10.1007/JHEP09\(2020\)143](#). arXiv: [2006.03056 \[hep-ph\]](#).
- [20] Daniel Baranowski et al. “Zero-jettiness soft function to third order in perturbative QCD.” In: (Sept. 2024). arXiv: [2409.11042 \[hep-ph\]](#).
- [21] Daniel Baranowski et al. “Triple real-emission contribution to the zero-jettiness soft function at N³LO in QCD.” In: (Dec. 2024). arXiv: [2412.14001 \[hep-ph\]](#).
- [22] John M. Campbell et al. “The NNLO QCD soft function for 1-jettiness.” In: *Eur. Phys. J. C* 78.3 (2018), p. 234. DOI: [10.1140/epjc/s10052-018-5732-1](#). arXiv: [1711.09984 \[hep-ph\]](#).
- [23] Thomas Becher and Guido Bell. “The gluon jet function at two-loop order.” In: *Phys. Lett. B* 695 (2011), pp. 252–258. DOI: [10.1016/j.physletb.2010.11.036](#). arXiv: [1008.1936 \[hep-ph\]](#).
- [24] Thomas Becher and Matthias Neubert. “Toward a NNLO calculation of the anti- $B \rightarrow X(s)$ gamma decay rate with a cut on photon energy. II. Two-loop result for the jet function.” In: *Phys. Lett. B* 637 (2006), pp. 251–259. DOI: [10.1016/j.physletb.2006.04.046](#). arXiv: [hep-ph/0603140](#).
- [25] Radja Boughezal, Xiaohui Liu, and Frank Petriello. “ N -jettiness soft function at next-to-next-to-leading order.” In: *Phys. Rev. D* 91.9 (2015), p. 094035. DOI: [10.1103/PhysRevD.91.094035](#). arXiv: [1504.02540 \[hep-ph\]](#).
- [26] M. Czakon. “A novel subtraction scheme for double-real radiation at NNLO.” In: *Phys. Lett. B* 693 (2010), pp. 259–268. DOI: [10.1016/j.physletb.2010.08.036](#). arXiv: [1005.0274 \[hep-ph\]](#).
- [27] Michał Czakon et al. “Single-jet inclusive rates with exact color at $\mathcal{O}(\alpha_s^4)$.” In: *JHEP* 10 (2019), p. 262. DOI: [10.1007/JHEP10\(2019\)262](#). arXiv: [1907.12911 \[hep-ph\]](#).